Undersampling Reference Receiver For LNA Distortions Compensation Direct RF Digitization Receiver

Ngoc-Anh Vu[1], Thi-Hong-Tham Tran[2], Hai-Nam Le[1], Hai Duong Nguyen [1], Quang-Kien Trinh[1]
[1]Le Quy Don Technical University, 236 Hoang Quoc Viet Str., Hanoi, Vietnam
[2]Moscow Institute of Physics and Technology, Moscow, Russia
Email: tranhongtham@phystech.edu, anhvn@lqdtu.edu.vn

***Abstract*— The paper analyzes the effect of the nonlinear distortion of Low Noise Amplifier (LNA) in multichannel direct RF digitization receivers (DRF–RX). A novel distortion compensation approach has been proposed, where the compensation is performed entirely in the digital domain at baseband after the digital down-converter (DDC). Distortion information is extracted from the signals of the main receiver and a linear reference receiver. The reproduced information is used for distortion compensation using a nonlinear model and an adaptive Least Mean Square (LMS) algorithm. As the major advantage, processing at baseband with a low sampling rate significantly reduces the cost, the design complexity and the energy consumption of the receiver. The proposed undersampling reference receiver structure exhibits additional benefit in terms of hardware usage and energy consumption by using a low-cost and large dynamic range ADC. To verify the scheme's efficiency, an Ultra High Frequency (UHF) DRX with four QPSK channels is simulated by Matlab Simulink. The simulation results show that the method improves the Spurious-free dynamic range (SFDR) with an increase of about 20 dB, compared to the results of RX without distortion compensation.**

Keywords— Direct RF digitization, DCR, LNA distortion, digital receiver, LMS filter, multichannel receiver, software-defined radio, UHF transceiver.

I. Introduction

DIRECT conversion receiver (DCR) is becoming a popular architecture in the design of the next radio receivers generation [1]–[6]. DCRs exhibit a number of advantages, architectural simplicity, supporting multiple functions and upgradability [4]–[6]. Among DCR, DRX is a fully digital receiver architecture, where the radio frequency (RF) signal is sampled directly by a high-speed ADC, which allows all processing can be done in the digital domain. High-sampling ADCs are vital in this type of receiver, and the unavailability of such ADCs is the main obstacle preventing this architecture in the practice. Nonetheless, the DRX with such ADC dynamic range still needs an LNA in order to achieve the required level of sensitivity. Therefore, DRXs still suffer from the unavoidable non-linearity comes from LNA.

When working in multi-channel mode, the multi-channel receiver allows the simultaneous receiving of multiple channels with different types of signal modulation and power levels [7]-[11]. In such a condition, it is inevitable that after being amplified by the LNA, high energy channels generate nonlinear distortions. These distortions, in turn, degrade the signal quality of the nearby channels [7]–[11]. The higher the power of distortion channels, the more serious the effect of LNA nonlinearity is, and this essentially requires advanced technique and post-processing algorithms in the digital domain.

Studies in nonlinear distortion compensation have been actively carried out [7]–[11]. These studies adopted either Hammerstein's model [8]–[11] or Volterra series [7] to mathematically analyze the LNA nonlinearity. The main solutions for distortion compensation are canceling or inverting the nonlinear components. Accordingly, in either approach, estimating the distortion components is the fundamental task of all methods.

Solutions in [7] and [11] use a band-pass filter (BPF) to extract the information for the distortion estimation. In [10], the distortion is evaluated using a part of distorted information from the high-frequency BPF. However, this method is not very practical due to the high complexity designing such BPF. Similarly, a BPF is also used in [11] to extract the distortion signals, but this solution requires that the information of the channel causing distortion needs to be known in advance.

A solution using a secondary reference receiver to reproduce and suppress distortion is proposed in [8]. However, the distortion compensation is carried out at the high-frequency domain and the technique was applied for common DCRs with existing non-linear distortion components from the analog sub-circuit (i.e., quadrature mixers). Thus, the compensation circuit was highly complex and energy consuming.

In this work, the impacts of the LNA's nonlinearity on DRF–RX are systematically studied in detail. We then propose a novel approach to tackle the distortion issues in multichannel DRF–RX. Our approach based on a feed-forward compensation circuit that can real-time and continuously extract and detect the distortion component globally without knowing in advance the RF signals' characteristics. The main distinguishing feature of our approach from the prior arts is that the distortion compensation is performed at low frequency instead of at RF domain that essentially simplifies the compensation circuit and reduces the hardware cost.

The reference channel requires only a low-speed ADC to extract sufficient information for distortion reconstruction thanks to the undersampling effect. This technique overcomes certain drawbacks of prior arts in power consumption and device cost. It thus is well suited for mobile/handheld communication devices, where power consumption and compactness could be the primary concerns.

The remaining of the paper is organized as follows. Section II presents distortion models of LNA and analyzes the effect of distortion on the multichannel DRX model. Section III proposes the solution to compensate LNA's distortions. Conclusions are drawn in section IV.

II. NONLINEAR LNA DISTORTIONS MODELS IN DRXS

A. RF Nonlinear Distortion Model

The generic structure of DRX is shown in Fig. 1. An array of BPFs is still required in order to attenuate the out-of-band frequencies [2]. Then, the filtered signal is going through an LNA before being digitalized by a high-speed ADC, which has to support from a few hundred to GHz frequency range. Even though the receiver is equipped with the most advanced ADCs, those ADCs could offer the resolution as high as 14 bits [13, 14], which corresponds to an approximate SFDR of 86 dB [15]. To ensure the receiver sensitivity of approximate -100 dBm, the signal would need to be amplified by about 20 dB. Hence, the LNA is an indispensable component in any DRX designs [3], [11] and the LNA nonlinearity effects are unavoidable. Note that even when higher dynamic range ADCs become available, distortion compensation techniques are still essential for achieving the cost-effective and low-power consumption design.

There are two types of nonlinear LNA distortions that need to be taken into consideration: self-affected distortions caused by an individual RF signal to itself and distortions causes by the interference of other RF signals [3], [14]. The model of nonlinear components is assumed to be a polynomial with the form

$$y_{RF}(t) = a_1(t)x_{RF}(t) + a_2(t)x_{RF}^2(t) + a_3(t)x_{RF}^3(t) + \cdots + a_{\mathrm{n}}(t)x_{RF}^{\mathrm{n}}(t) \quad (1)$$

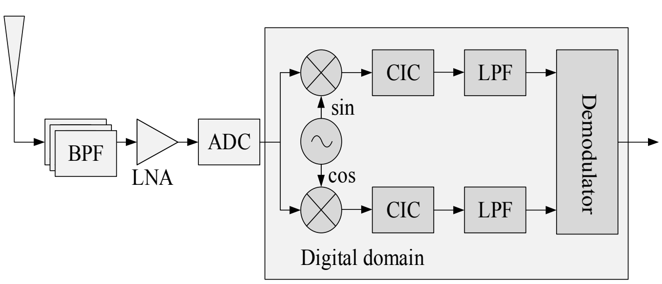

Fig. 1. The architecture of direct digitization receiver

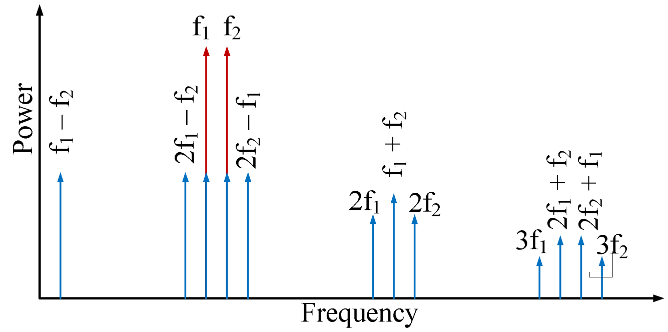

Fig. 2. The nonlinear components of LNA with two-tone input

where $x_{RF}(t)$ and $y_{RF}(t)$ are LNA input and output signals respectively; $a_{\mathrm{i}}(t)$ is the i$^{\mathrm{th}}$-order component coefficient. The input signal $x_{RF}(t)$, in turn, is represented as

$$x_{RF}(t) = 2Re[x(t)e^{j\omega_c t}] = x(t)e^{j\omega_c t} + x^* e^{-j\omega_c t} \quad (2)$$

where $x(t)$ is the baseband signal of $x_{RF}(t)$, $x(t)$ can be a single carrier frequency or multiple separate carrier frequencies. $\omega_c = 2\pi f_c$, with f_c is the center carrier frequency and (.)* represents the complex conjugate operator.

As illustrated in Fig. 2. , when the input signal has two frequencies components (f_1, f_2), the output signal will have two harmonic groups: $n \times f_1$, $m \times f_2$, and inter-modulation $n \times f_1 \pm m \times f_2$. The distortion happens as soon as those components appear near the received signal frequency. For example, components $(2f_1 - f_2)$ and $(2f_2 - f_1)$ could distort f_1 and f_2. The other harmonics and inter-modulation, on the other hand, could distort other high-frequency signals.

B. Baseband Nonlinear Distortion Model

With the DRX structure shown in Figure 1, assume that $2f_c \gg BW$ (bandwidth), a significant number of out-of-band signals will be removed after the digital downconverters. This is because the DDC acts as an LPF, which shifts the RF signal to the baseband. Correspondingly, the expression of (1) can be greatly simplified. The quadratic component in (1) is expressed as

$$x_{RF}^2(t) = 2A^2(t) + x^2(t) \cdot e^{2\omega_c t} + [x^*(t)]^2 \cdot e^{-j2\omega_c t} \quad (3)$$

where $2A^2(t) = 2x(t) \cdot x^*(t)$ is the spectral content around the DC component. From (3), distortion frequencies appear at 0 and $\pm 2\omega_c$but there is no frequency component at ω_c. Similar discussion can be found for other even order components. Therefore, all even-order harmonics in (1) are eventually phased out after the DDC. Similarly, other high-frequency distortion components will not appear at reception bandwidth and can be excluded.

Therefore, in DRXs, LNA's non-linearity is most severe at only odd-order components because their generated distortions could locate around ω_c. In practice, it is sufficient to take into consideration up to the third-order components because higher-order components often have very small energy.

Therefore, the simple RF non-linear model can be written as

$$y_{RF}(t) = a_1 x_{RF}(t) + a_3 x_{RF}^3(t) \quad (4)$$

Here a_1 is the linear gain of LNA, and a_3 is the distortion coefficient of the third-order component. The impact of LNA non-linearity distortion components, that affect DRX, are illustrated in Fig. 3. As can be seen from the figure, the third-order intermodulation of f_1, f_2 produce frequencies (i.e., $2f_1 - f_2$, $2f_2 - f_1$), which are closed to f_3, f_4 and f_5 interfere channels at these positions. Higher harmonic and intermodulation are filtered out at moderate BW of the UHF receiver. From (2), the third-order component in (4) can be written in full form as

$$\begin{aligned} a_3 x_{RF}^3(t) \\ &= a_3\{x^3(t)e^{j3\omega_c t} + [x^*(t)]^3 \cdot e^{-j3\omega_c t} + 3A^2(t) \\ &\cdot x(t)e^{j\omega_c t} + 3A^2(t)x^*(t)e^{-j\omega_c t}\} \end{aligned} \quad (5)$$

After I/Q downconversion, all high-frequency components (at $3\omega_c$) are removed, the remaining components in (5) is $3A^2(t) \cdot x(t) \cdot e^{j\omega_c t}$ and $3A^2(t) \cdot x^*(t) \cdot e^{-j\omega_c t}$. Hence, the baseband equivalence of the LNA non-linear model for DRX (4) is reduced to be

$$\begin{aligned} y_{BB}(t) &= y_{BB,I}(t) + j \cdot y_{BB,Q}(t) \\ &= a_1 \cdot x(t) + 3a_3 \cdot A^2(t) \cdot x(t) \end{aligned} \quad (6)$$

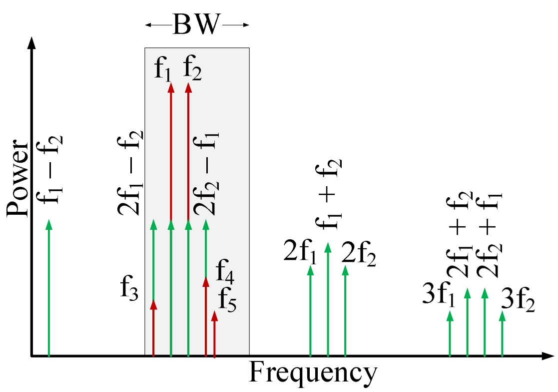

Fig. 3. Distribution of the distortion frequencies according to model in (5)

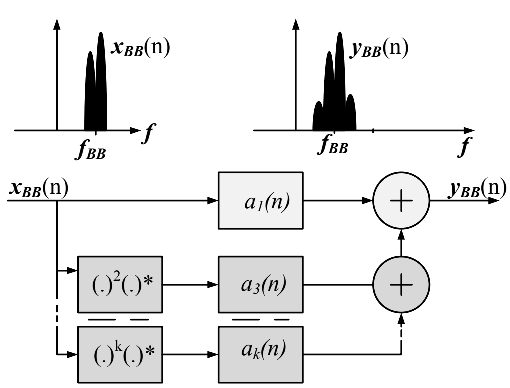

Fig. 4. A reduced non-linear model of LNA in multi-channel DRXs after the DDC.

where,

$$y_{BB,I}(t) = a_1 \cdot x_I(t) + 3a_3 \cdot A^2(t) \cdot x_I(t) \quad (7)$$

$$y_{BB,Q}(t) = a_1 \cdot x_Q(t) + 3a_3 \cdot A^2(t) \cdot x_Q(t) \quad (8)$$

From (7)–(8), the distortion model at the baseband is much simpler compared to the model in the RF domain. The non-linear component $3a_3 \cdot A^2(t) \cdot x(t)$ essentially causes intermodulation in the frequency range around ω_c. The corresponding non-linear model and an example spectrums are illustrated in Fig. 4. Ideally, all high order-component are filtered by DDC and the spectrum of $x_{BB}(t)$ are shown in the left. However, due to the effect of intermodulation, the actual baseband spectrum (y_{BB}(t)) is shown in the right where new third-order distortions components appear near the interested frequencies.

The derived models (7)–(8) in this Section will be used as the fundamental ground for designing the distortion compensation circuit for the DRXs, which is presented in the subsequent Section.

III. Proposed Distortion Compensation Scheme For Multichannel DRXs

A. Distortions Compensation Circuits Using The Undersampling Technique

In this section, we propose a novel after-DDC distortion compensation scheme for DRX. The structure of the proposed RX comprises the main receiver and a reference receiver depicted in Fig. 5. The former still needs an LNA to ensure good sensitivity as discussed before, while the latter is designed without LNA so that the received signals remain linear. The reference receiver uses an ADC combining with an undersampling technique [15] to extract the distortion information.

The structure of the DRX using this approach is shown in Fig. 5. Accordingly, the sampling rate of the reference ADC is two times smaller than the maximum frequency of the signal but more than twice the signal bandwidth. With this solution, to avoid unwanted aliasing in the reference receiver, a BPF (BPF2 in Fig. 5) before ADC is required. The BPF's bandwidth is equal to the frequency range of the main receiver. It is worthwhile to note that, applying directly undersampling for the main receiver is theoretically feasible. However, the RF analog BPF must have much higher quality, compared to the digital reference receiver BPF, in order to eliminate unwanted aliasing. It leads to a number of practical

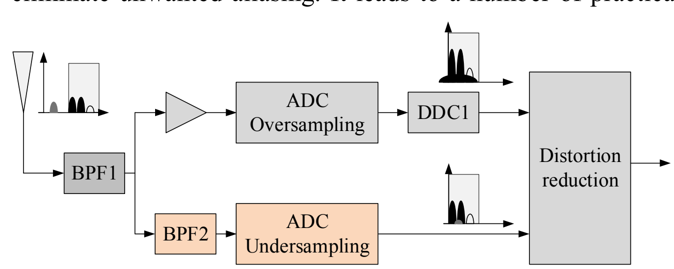

Fig. 5. The structure of multichannel DRXs with the proposed distortion compensation circuit

difficulties and extra design cost. Therefore, in the main receiver channel, high-speed ADC is still needed, and the sampling frequency is much higher than the signal bandwidth.

With our proposal, the ADC sampling rate needs to be at least two times higher than the receiver's bandwidth [16]. If W is the receiver's bandwidth ($W = f_{High} - f_{Low}$) then the required sampling frequency is $f_s \geq 2W$ and:

$$\frac{2f_{High}}{n} \leq f_s \leq \frac{2f_{Low}}{n-1} \tag{9}$$

With any integer n satisfying:

$$1 \leq n \leq \left(\frac{f_{High}}{f_{High} - f_{Low}}\right) \tag{10}$$

Since there is no DDC in the reference receiver, the two receivers are out of sync. To synchronize these receivers, a delay tap is added to the reference receiver. The delay time depends on the actual design of the receiver and it should be tuned based on the switching time of ADC processing time and low-speed DDC. Such delay stage is not an issue when implementing in the digital domain.

B. LNA nonlinear Distortion Reproduction

As analyzed in Section II, due to LNA's nonlinearity, high energy signal channels entering the receiver creates distortion components. Based on the model in (7)–(8), by exploiting the downconverting function of the downconverter, for DRX, we could perform distortion canceling after DDC, i.e., at low sampling rate domain.

Assuming the baseband signal received from the antenna after going through LNA, ADC and DDC is

$$\begin{aligned} y_{BB}[n] &= w_1 f_1(x_{BB}[n]) + w_3 f_3(x_{BB}[n]) \\ &= x_{BB}[n] + e[n] \end{aligned} \tag{11}$$

where n is sampling sequence number, $f_1(x_{BB}[n]) = x_{BB}[n]$ is the linear component and $f_3(x_{BB}[n]) = x_{BB}^3[n]$ are the second and third-order components. $w_i[n]$ is the i^{th}-order coefficient. Accordingly, the distortion components in (9) are

$$e[n] = w_3[n] \cdot f_3(x_{BB}[n]) \tag{12}$$

From the linear reference channel, the reproduced distortion $\hat{e}[n]$ is expressed as

$$\hat{e}[n] = \widehat{w}_3[n] \cdot f_3(x_{BB}[n]) \tag{13}$$

The distortion canceling circuit (see Fig. 5) subtracts the reproduced distortion components of the linear channel from the distorted signal after the main receiver DDC, hence

$$\hat{x}_{BB}[n] = y_{BB}[n] - \hat{e}[n] \tag{14}$$

From (11), (13) and (14) the final output signal is rewritten as

$$\begin{aligned} \hat{x}_{BB}[n] &= x_{BB}[n] + e[n] - \hat{e}[n] \\ &= x_{BB}[n] + (w_3[n] - \widehat{w}_3[n]) \cdot f_3(x_{BB}[n]) \end{aligned} \tag{15}$$

From (15) it can be seen that the signal after distortion compensation $\hat{x}_{BB}[n]$ is equal to $x_{BB}[n]$ as long as high-order coefficients $\widehat{w}_3[n]$ in (13) are the same as those $w_3[n]$ in (12). By adopting the LMS algorithm, the coefficients of the nonlinear model are determined as follows:

$$\begin{aligned} \widehat{w}_1[n] &= \widehat{w}_1[n-1] + \mu_1 \cdot f_1(x[n]) \cdot \hat{\varepsilon}[n] \\ \widehat{w}_3[n] &= \widehat{w}_3[n-1] + \mu_3 \cdot f_3(x[n]) \cdot \hat{\varepsilon}[n] \end{aligned} \tag{16},$$

where $\hat{\varepsilon}[n]$ and μ_i $\{i = 1 - 3\}$ are LMS algorithm parameters; $\hat{\varepsilon}$ is estimation error and is expressed as $\hat{\varepsilon}[n] = y[n] - \big(\widehat{w}_1 \cdot f_1(x[n]) + \widehat{w}_2 \cdot f_2(x[n]) + \widehat{w}_3 \cdot f_3(x[n])\big)$; μ_i are the LMS algorithm step sizes.

C. Evaluation of The Proposed Distortion Compensation Technique

To evaluate the effect of the proposed distortion reduction techniques, we implemented the UHF DRXs model which can receive multiple channels simultaneously from 900 MHz to 1000 MHz. We simulated four QPSK channels with each channel data rate is 4 Mbps. One channel is outside the receiver's range and the other three are within the receiver's band.

The detailed channels parameters are specified in TABLE I.

TABLE I
SIMULATION PARAMETERS

RF input	Before DDC	After DDC
Channel 1, QPSK, 4 Msps*, -55dBm	f_{RF1} = 919.5 MHz	f_1 = 23.5 MHz
Channel 2, QPSK, 4 Msps*, -55dBm	f_{RF2} = 930.0 MHz	f_2 = 34.0 MHz
Channel 3, QPSK, 4 Msps*, -85dBm	f_{RF3} = 940.5 MHz	f_3 = 44.5 MHz
Channel 4, QPSK, 4 Msps*, -55dBm	f_{RF4} = 865.5 MHz	f_4 = 30.5 MHz

*Msps = Mega samples per second.

The baseband spectra before and after the distortion correction are shown in Fig. 6. The baseband frequency are $f_{1,BB} = 23.5$ MHz, $f_{2,BB} = 34$ MHz, and $f_{3,BB} = 44.5\ MHz$). The input power levels of f_1 and f_2 are intentionally set to be -55 dBm, which are higher than f_3 (-85 dBm). Thus, f_1 and f_2 will act as the aggressor channels. Intermodulation distortions from these two channels will appear around f_1, f_2 themselves and also around f_3. As shown in Fig. 6, the spectrum after the compensating process is greatly improved from the effects of nonlinear distortion. The nonlinear components (green line) generated by f_1 and f_2 are effectively reduced.

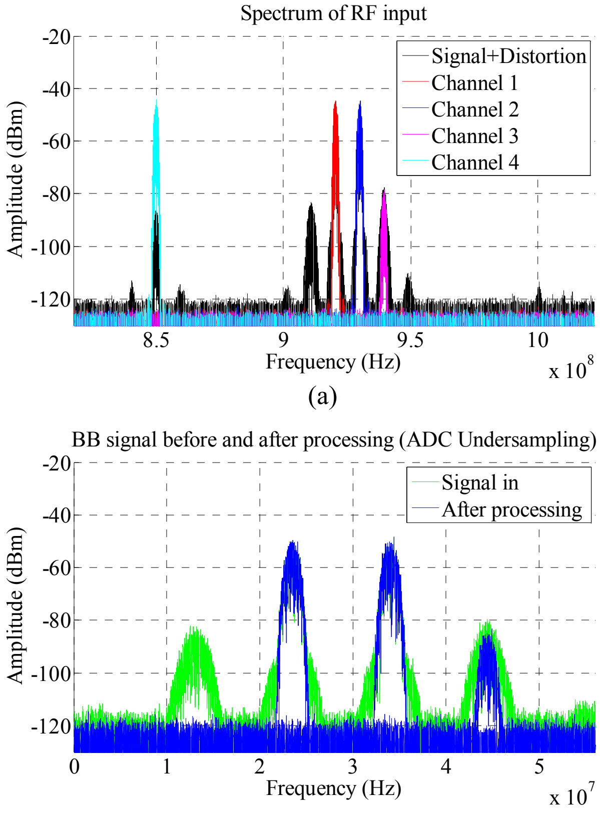

(b)

Fig. 6. (a) Spectra of received signals; (b) Spectra of targeted signals before and after distortion compensation using the undersampling technique

IV. CONCLUSIONS

In this paper, the impacts of LNA distortions on DRXs have been systematically studied in detail. From the derived signal analytical models, we have proposed a novel distortion compensation scheme for DRXs that allows shifting all processes into the low-frequency domain. The solution with undersampling ADC for the reference channel has been implemented and verified by Matlab via a DRXs configured with four 4-Mbps QPSK channels. The simulation results indicated that the implemented compensation schemes effectively improve the received signal SFDR by 20 dB. The proposed schemes can blindly remove all types of distortions and all the processing is done at the baseband. These schemes are beneficial in terms of hardware usage, energy and simplify the receiver design. Although an additional BPF is required, this scheme has an obvious advantage in hardware usage, cost, and power consumption and can be a favorite option for energy- and area-constrained devices.

REFERENCE

[1] Software Defined Radio, Spectrum Analyzer, and Panoramic Adapter/ Available: http://www.rfspace.com/RFSPACE/SDR-IQ.html. [Accessed May 20, 2019].

[2] Perseus SDR - Software Defined 10 kHz - 30 MHz Receiver. Available: http://microtelecom.it/perseus/. [Accessed May 20, 2019].

[3] O. Jamin, *Broadband Direct RF Digitization Receivers*, Analog Circuits and Signal Processing 121, DOI 10.1007/978-3-319-01150-9_2, Springer International Publishing Switzerland 2014

[4] A. A. Abidi, "Direct-conversion radio transceivers for digital communications," *IEEE J. Solid-State Circuits*, vol. 30, no. 12, pp. 1399–1410, Dec. 1995.

[5] O. Jamin, V. Rambeau, F. Goussin, and G. Lebailly, "An rf frontend for multi-channel direct rf sampling cable receivers," in *ESSCIRC (ESSCIRC), 2011 Proceedings of the*, Sept 2011, pp. 347–350.

[6] B. Razavi, "Design considerations for direct-conversion receivers," *IEEE Trans. Circuits Syst. II, Analog Digit. Signal Process.*, vol. 44, no. 6, pp. 428–435, Jun. 1997.

[7] R. Vansebrouck, O. Jamin, P. Desgreys, and V.-T. Nguyen, "Digital distortion compensation for wideband direct digitization RF receiver," *in Proc. IEEE 13th Int. New Circuits Syst. Conf. (NEWCAS),* Jun. 2015, pp. 1–4.

[8] Jaakko Marttila, Markus Allénand Marko Kosunen, "Reference Receiver Enhanced Digital Linearization of Wideband Direct-Conversion Receivers" *IEEE Transactions On Microwave Theory And Techniques*, vol.65, no. 2, pp. 607-620, February 2017

[9] M. Allén, J. Marttila, M. Valkama, S. Singh, M. Epp, and W. Schlecker, "Digital full-band linearization of wideband direct-conversion receiver for radar and communications applications," in *Proc. 49th Asilomar Conf. Signals, Syst. Comput.*, Pacific Grove, CA, USA, Nov. 2015, pp. 1361–1368.

[10] Raphaël Vansebrouck, Chadi Jabbour, Olivier Jamin, and Patricia Desgreys, "Fully-Digital Blind Compensation of Non-Linear Distortions in Wideband Receivers" *IEEE Transactions OnCircuits And Systems-I: Regular Papers*, vol. 64, no. 8, pp. 2112-2123, August 2017.

[11] M. Grimm, M. Allen, J. Marttila, M. Valkama, and R. Thoma, "Joint mitigation of nonlinear rf and baseband distortions in wideband direct-conversion receivers," *Microwave Theory and Techniques, IEEE Transactions on*, vol. 62, no. 1, pp. 166–182, Jan 2014.

[12] Gharaibeh, Khaled M, *Nonlinear distortion in wireless systems: modeling and simulation with MATLAB*, John Wiley & Sons Ltd, 2012

[13] Texas Instruments. "ADC32RF83 Dual-Channel, 14-Bit, 3-GSPS, RF Sampling Wideband Receiver, and Feed," ADC32RF83 datasheet Available: http://www.ti.com/product/ADC32RF83

[14] Texas Instruments. "ADC32RF45 Dual-Channel, 14-Bit, 3-GSPS RF-Sampling Analog-to-Digital Converter (ADC)," ADC32RF45 datasheet, Available: http://www.ti.com/product/ADC32RF45

[15] Purnachandar Poshala, "Why Oversample when Undersampling can do the Job?", *Texas Instruments Incorporated,* July 2013. Available: http://www.ti.com

[16] Rodger H. Hosking, Pentek, "How to use undersampling", Dec. 2006. Available: https://www.eetimes.com/document.asp?doc_id=1275354#